

## PALYNOFACIES, ORGANIC GEOCHEMICAL ANALYSES AND HYDROCARBON POTENTIAL OF THE TAKORADI 11-1 WELL, SALTPOND BASIN, GHANA

\*D. Atta-Peters<sup>1</sup>, C. A. Achaegakwo<sup>2</sup>, P. Garrey<sup>3</sup>

*Department of Earth Science, University of Ghana, P. O. Box LG 58, Legon, Accra, Ghana*  
*[\\*dattapeters@gmail.com](mailto:dattapeters@gmail.com)<sup>1</sup>, [chrisach007@yahoo.com](mailto:chrisach007@yahoo.com)<sup>2</sup>, [pgarrey@yahoo.com](mailto:pgarrey@yahoo.com)<sup>3</sup>*

Received July 13, 2015, Accepted November 23, 2015

---

### Abstract

Hydrocarbon potential of the rocks in Takoradi 11-1 well in the Saltpond Basin have been investigated. Palynological and organic geochemical analysis were carried out on 49 cutting samples and 18 core samples respectively. Palynofacies analysis of the Albian – Cenomanian sediments reveal three palynofacies associations: PA-1 reflects deposition in distal mud-dominated oxic shelf conditions, PA-2 and PA-3 deposition under distal dysoxic – anoxic outer and inner shelf respectively. Palynofloral association which is indicative of the Albian – Cenomanian elaterate province, has pteridophytic and xerophytic forms that reflect a palaeoenvironment which was moist and humid in a warm coastal plain under arid/semi-arid climatic condition.

Geochemical analysis shows low to moderate total organic content (TOC). It varies between 0.53 – 2.73 (ave 0.83 wt% TOC) and S<sub>2</sub> values 0.33 – 8.36 (ave. 1.32 mg HC/g rock) which implies a poor to fair source rock. Rock-Eval pyrolysis indicates mainly kerogen type III (gas prone) of hydrogen index (HI) values 53 – 387 (ave 135 mg HC/g TOC). The thermal maturation parameters, Tmax of values between 427 – 441 (ave 436.5 °C) and production index (PI) 0.02 – 0.15 (ave 0.06 mg HC/g rock) indicate that the rocks in the well are at immature to early mature stage oil window.

**Keywords:** Palynofacies; Kerogen; Palynomorphs; Hydrogen index; Thermal maturation; Production index.

---

### 1. Introduction

The Saltpond Basin is a Palaeozoic wrench modified pull-apart basin centrally located between the Tano-Cape Three Points and Accra-Keta (Fig. 1). Its total size is approximately 12,294 km<sup>2</sup> with 204km<sup>2</sup> onshore and 12,089 km<sup>2</sup> offshore. About 95% of the basin lies in shallow water. The Saltpond Basin is limited by the Precambrian basin at the north [31]. At the east, it is separated from the Benin embayment by a hinge line whereas at the western limit between Cote d'Ivoire and Saltpond basin, it appears to be an easterly/lateral sedimentary onlap. The Saltpond Basin is mainly characterized by sandstone and shale dominated formations with varied thicknesses. Structurally, the basin is quite complex, characterized by a network of faults which can ultimately displace individual units [22]. Gently rolling folds coupled with the faulted blocks provide the trapping conditions for the accumulation of expelled hydrocarbons into reservoir units. The only known and proven petroleum system in the basin is the lower Palaeozoic petroleum system. This system has Devonian source rocks (Takoradi shales) with Type II kerogen and moderate to good total organic carbon (TOC) and Hydrogen Index (HI). The Devonian to Carboniferous reservoir rocks are the Takoradi sandstone formations. Burial history construction and geochemical analysis indicate that the source rock was mature for hydrocarbon generation in the Middle Cretaceous [2,8,22].

## 2. Geology and tectonic setting

Offshore, Ghana is situated to the eastward extension of the Romanche and St Paul fracture zones which can be traced to the offset portion of the Mid-Atlantic Ridge. The Saltpond Basin is located on the northwest-southeast trending horst block which is characterized by numerous local faults [22]. These faults subdivide the horst into minor blocks. The horsts together with the grabens form a complex network of faults related to intercontinental rifting associated with transform marginal basins. The basin can be divided into five main genetic units based on age and associated geological events. (Table 1).

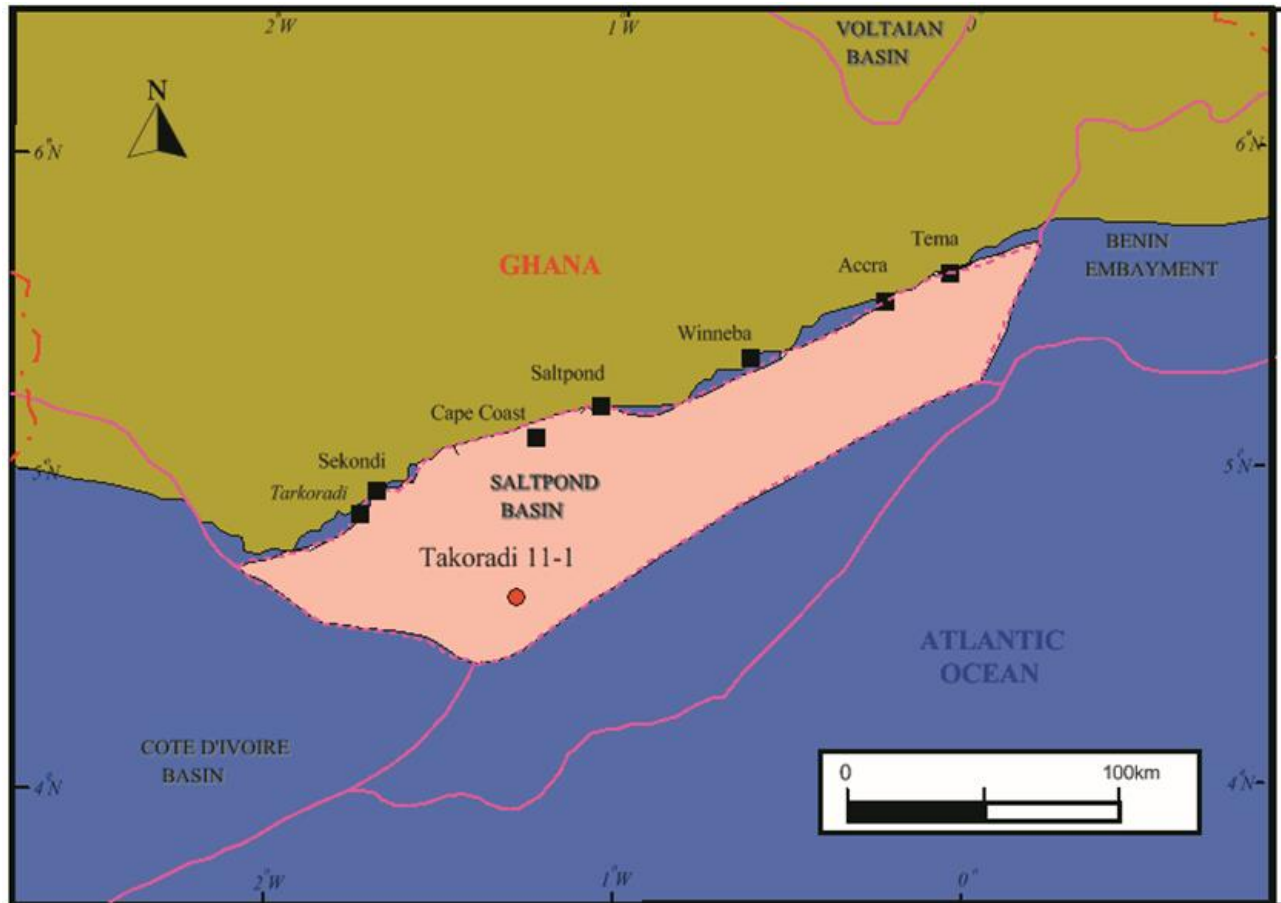


Fig. 1. Map of Saltpond basin showing Takoradi 11-1 well

Structurally, the Saltpond basin is located within the Takoradi Arch, one of the three provinces of Ghana's coastal basin [14]. According to [14], the arch on which the basin is located is represented by a series of tilted fault blocks striking north-northeast – south-southwest. This observation has been drawn from seismic sections of the basin derived from reflection seismic exploration.

The stratigraphic sequence in the Saltpond basin spans the ages of late Ordovician to early Cretaceous as typified by the rocks of the Sekondian Group (Fig. 2), with the oldest formation, Ajua Shales resting unconformably on the crystalline basement rock and the youngest being the Essikado sandstone.

Table 1 Genetic units of the Central basin (modified after [22])

Genetic unit	Age (million years)	Remarks
<b>Basement</b>	4000Ma-570Ma	Precambrian igneous and metamorphic rocks form the basement on which the Central basin is located.
<b>Intra-cratonic unit</b>	463.9Ma-208Ma	<p>This unit is characterized by deposits thought to be in an intra-cratonic tectonic regime at the time when the African and South American continental plates were still joined. Formations within this unit are as follows;</p> <ul style="list-style-type: none"> <li>• Ajua formation</li> <li>• Elmina formation</li> <li>• Takoradi formation</li> <li>• Sekondi formation</li> <li>• Efia Nkwanta formation</li> </ul> <p>The sequence is mainly composed of clastic rocks deposited in shallow marine to brackish water environments.</p>
<b>Pre-rift and initial rift</b>	178-167.1Ma	A minor clockwise rotation of the South American plate in relation to the African plate may have occurred as the South Atlantic ocean opened, instigating a dominantly extensional tectonic regime. The initial rifting of the plate began with the emplacement over a widespread area of volcanoclastics and doleritic sills and dikes. In Ghana, the age of these volcanics is dated between 162 Ma and 172 Ma [37].
<b>Syn-rift and wrench unit</b>	145.6Ma-97Ma	<p>Major east-northeast - west-northwest trending fracture zones, such as the Romanche and Chain fracture zones were formed as a result of the rifting of Africa and South America plate.</p> <p>In the Saltpond Basin, the Lower Cretaceous is characterized by thick, sandstone dominant formation deposited under continental environment.</p>
<b>Drift and passive margin</b>	97Ma-0Ma	Continental drifting began in Early Cenomanian and is identified by marine transgression deposits. Based on seismic and well data, the two most prominent unconformities are of Late Cretaceous and Eocene to Oligocene in age [37]. The Upper Cretaceous to Tertiary sequence is composed mainly of marine shales with subordinate sandstones [35].

### 3. Materials and method

Forty-nine (49) samples between intervals (5430-9750ft) from the Takoradi 11-1 well was obtained from Ghana National Petroleum Corporation (GNPC) core lab. They were prepared for palynomorphs following standard maceration techniques, using (35%) HCl and (40%) HF to digest the carbonates and silica contents of the samples. The residue was cleaned and centrifuged in ZnBr<sub>2</sub> (S.G. 2.0). The floating organic matter was sieved through 10 $\mu$  and 20 $\mu$  sieves. Permanent slides were prepared using glycerol gelatin as the mounting medium. All sample slides were studied using the Lecia DMEP 750 microscope.

Quantitative analysis of the overall kerogen composition was carried out by counting 400 particulate organic matter and palynomorphs to determine relative abundances in percentage of kerogen (Appendix 1, 2). These were then subjected to cluster analysis (Q-mode) using the computer programme SPSS (version 20). This cluster analysis forms discrete

groupings that are based on the percentages of kerogens and are thus displayed in a dendrogram (Fig. 3).

TOC and Rock Eval pyrolysis data from 18 core samples was provided by GNPC using Rock Eval II Pyrolyzer. All geochemical results used for the interpretation are listed in Appendix 3

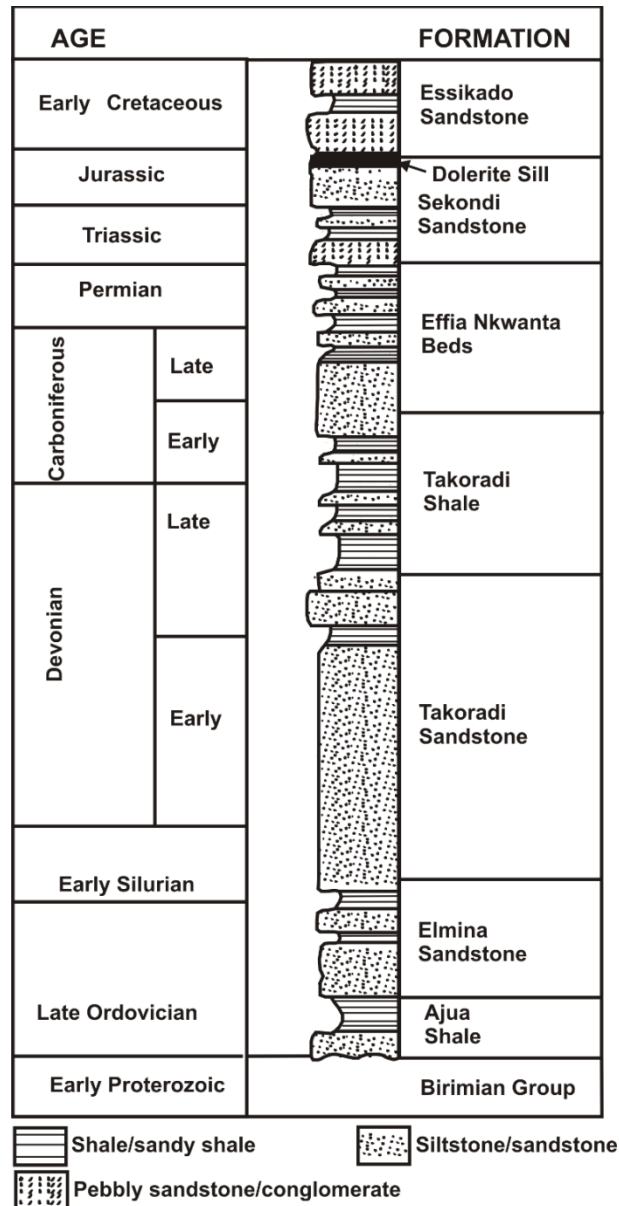


Figure 2 Stratigraphic sequence in the Saltpond Basin (modified after [5])

## 4. Results and discussion

### 4.1 Palynofacies analysis and palaeoenvironment

Palynofacies analyses is widely used for studying and explaining organic facies patterns. They permit recognition of sedimentary organic matter (SOM) and in addition describing processes that are contemporaneous or later to formation of the SOM which assists in hydrocarbon source rock evaluation [10,11,55] identified four main constituents of SOM; palynomorphs, phytoclasts, opaques, and amorphous organic matter (AOM). Palynofacies analyses

involves the identification of these groups, their absolute and relative proportions, sizes and preservation rates [54,55]. Being based on optical observation of organic particles present in sedimentary rocks, it provides more variables upon which to base determinations of sedimentary environments [10,55]. Cluster analysis (Q-mode), discriminated three discrete groupings (palynofacies type) based on the percentages of kerogens (Fig. 3; Table 2; 3). The AOM-Palynomorphs-Phytoclasts (APP) ternary plot [55] (Fig. 4) was used to identify depositional environment. Palynomorphs have environmental connotation and can thus be used to infer palaeoclimatic and palaeoenvironmental characteristics [55].

#### **4.1.1. Palynofacies assemblage 1 (PA-1). Relatively equal dominance of Palynomorphs and AOM. Plate III Fig. A, B**

PA-1 occurs at sample depths (ft) 7860, 8310, 7770, 9390, 9210, 8670, 8760, 8400, 8580, 8490, 6150, 8220, 6060, 9300, 5880, 8040, 8130, 5970, 5430, 5700, 8940, 9030, 7950, 7230, 7320, 5610, 9120, 5520 and 6240. It is made up of relatively equal dominance of AOM (30%) and palynomorphs (32%) with phytoclasts (26%). Opaques have relative abundance of 12%. The palynomorph group is characterized solely by terrestrial palynomorphs. On the APP ternary diagram of [55], PA-1 plots in field V which reflects distal mud-dominated oxic shelf conditions. This facies is attributed to shallow marine – nearshore environment. The fact that terrestrial elements are abundant with the presence of almost structureless woody particles, and the absence of marine palynomorphs, it is likely that the AOM from PA-1 is from terrestrial origin. The absence of marine microplanktons might imply terrestrial conditions, but could equally reflect a strong dilution of marine elements by terrestrial organic input [21]. The opaques are most likely derived by the oxidation of translucent phytoclast materials during transport.

#### **4.1.2. Palynofacies assemblage 2 (PA-2). AOM dominant. Plate III, Fig. C, D**

PA-2 is concentrated at sample depths (ft) 9480, 9570, 9660 and 9750. AOM dominates the total organic matter composition of this palynofacies (up to 45% of total organic matter). The high abundance of AOM is the result from the combination of environments with high preservation rates and low energies in reducing basins, with increased water column resulting in dysoxic or anoxic bottom condition. [12, 30, 36, 54, 55]. Phytoclasts (28%) also support the suggested offshore setting, where irrelevantly low concentrations were equated to weak terrestrial influx and deposition in distal settings located far from land vegetation [4]. The presence of terrestrial palynomorphs (14.5%) indicates input from a river or transport from a nearshore environment. Marine microplanktons (0.5%) are rare, this reflects a relatively nearshore marine influence. This palynofacies association (PA-2) plots in the field VII of the APP diagram thus supporting deposition in a distal dysoxic – anoxic shelf environment, located relatively far from high terrestrial organic matter input.

#### **4.1.3 Palynofacies assemblage 3 (PA-3). Palynomorphs dominant with phytoclasts and AOM. Plate III, Fig. E, F.**

PA-3 occurs at sample depths (ft) 6960, 7050, 6510, 7410, 7140, 6330, 6600, 6690, 7500, 5790, 6780, 6870, 6420, 8850, 7590 and 7680. It is characterized by high percentage of palynomorphs (44%) mainly spores and pollen and phytoclast (27%). This palynofacies is dominated by terrestrial elements with no marine palynomorphs. The dominance of miospores (terrestrial palynomorphs) may suggest that deposition might have taken place in the vicinity of an active fluvio-deltaic environment with proximity to source or nearshore [16, 21]. AOM (23%) is moderately preserved with opaques making up 6% of total organic matter. The low amounts of opaques in PA-3 suggest low salinity due to close proximity to fluvio-deltaic sources [36]. It is also characterized by nearly equal percentages of phytoclast and AOM (27% and 23% respectively) which is indicative of shallow marine to nearshore environment [3]. On the APP ternary diagram, PA-3 plots in field VII which is interpreted to indicate deposition in distal dysoxic – anoxic shelf condition [55]. The higher occurrences of terrestrial

palynomorphs and lower abundance of AOM present in PA-3 relative to that in PA-2 indicate deposition in shallower (inner shelf) marine conditions close to land vegetation.

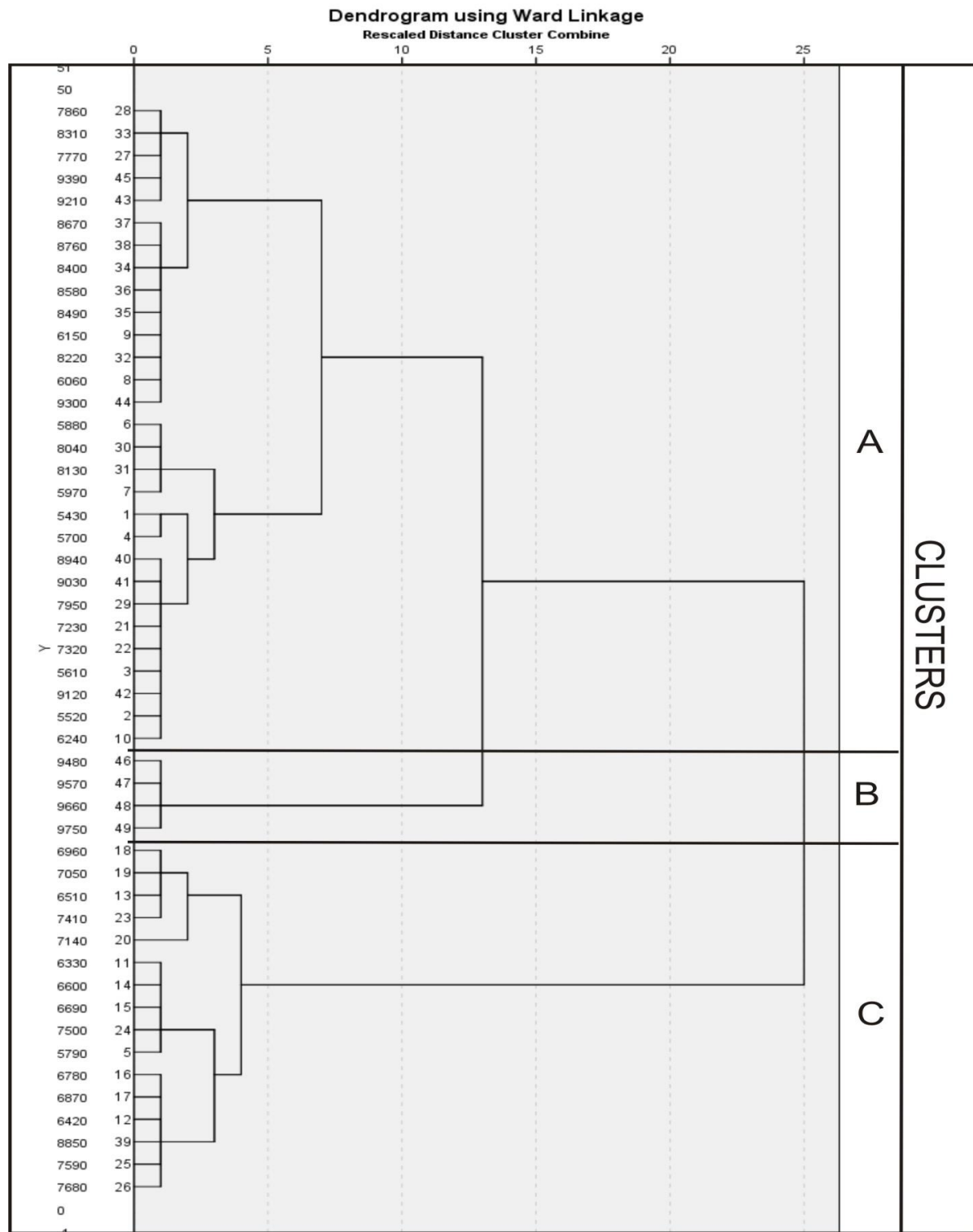


Fig. 3 Dendrogram by Q-mode of Takoradi 11-1 well shows the grouping of samples

Table 2 Palynofacies associations identified after cluster analysis

Palynofacies Types	Description	Cluster
PA-1	Relatively equal dominance of palynomorphs and AOM	A
PA-2	AOM dominant	B
PA-3	Palynomorphs dominant with phytoclast and AOM	C

Table 3 Palynofacies types and their percentages relative abundance of total kerogen.

Palynofacies type	AOM	Phytoclasts	Opaques	Palynomorphs
PA-1	30	26	12	32
PA-2	45	28	12	15
PA-3	23	27	6	44

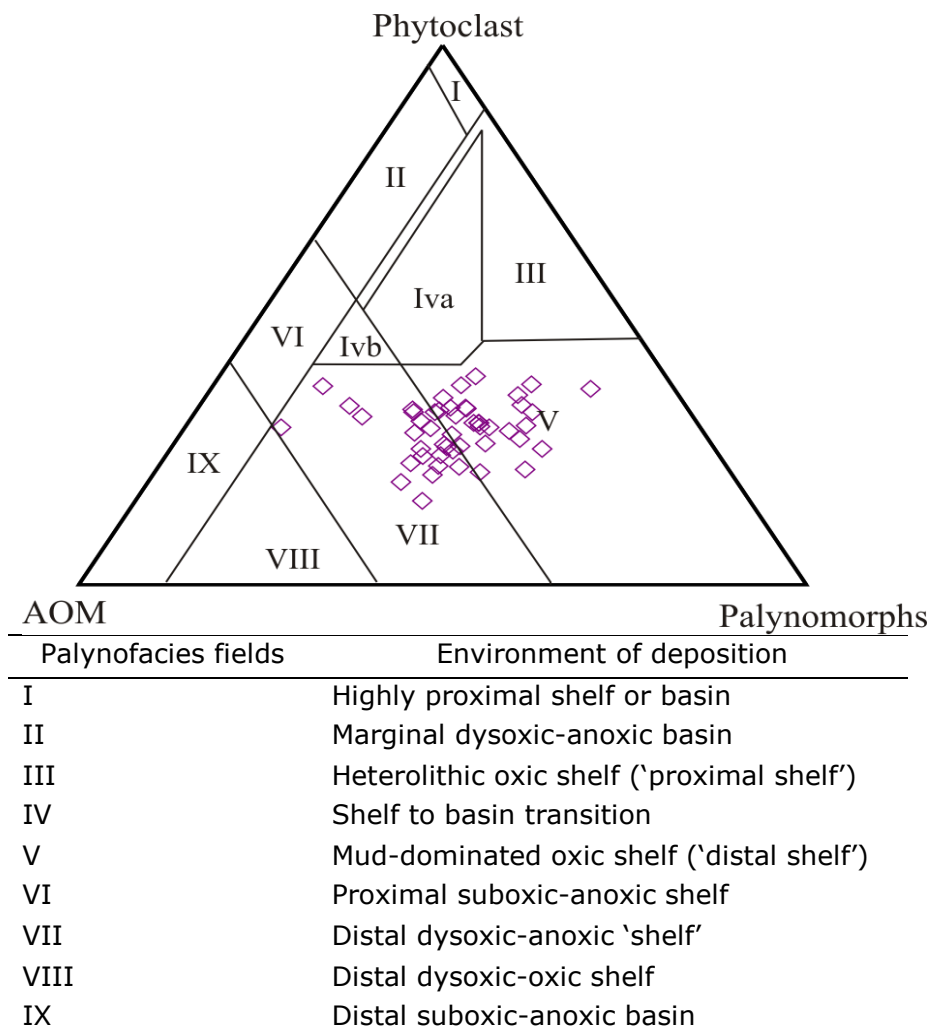


Fig. 4 A ternary APP palynofacies diagram with lower box showing key to palynofacies fields indicated on in the original diagram. (after [54])



## 5. Palaeoclimate and palynofloral province

The interval under study (5430-9750ft) is characterized by elater-bearing forms which are stratigraphically restricted to the Albian – Cenomanian Elaterate Province in the Africa-South America (ASA) region [1, 6, 13, 23-24, 26-27, 29, 33-34, 39, 44, 46, 51]. This province is characterised by the absence of bi- and trisaccate pollen, low abundances of fern spores, the presence of ephedroid complexes, *Classopollis* in association with *Afropollis* and frequent elater-bearing pollen and high percentages of angiosperm pollen. *A. jardinus*, *R. polymorphus* and *Classopollis classoides* which are associated with the elater forms in this interval have been reported from Aptian – Cenomanian age and are not found in sediments younger than the Cenomanian. The distribution of these characteristic elements paralleled the palaeolatitude and the axis of the Elaterate Province approximates the palaeoequator [25].

The abundance of the pteridophytic spores (eg. *Cicatricosisporites*, *Deltoidospora*, *Cyathidites*, *Concavisporites*) in most of the samples is attributable to vegetation growing on wetland such as riversides and coastal areas under fairly humid conditions [43, 45, 49]. These conditions are important for the production and transportation of resinous material (SOM) of high hydrogen index which is essential for hydrocarbon production.

The equally high percentage of elater pollen and *Afropollis* is an indication of their parent plants inhabiting humid coastal plains [15, 38, 47]. The elaterates and associated xerophytes (*Classopollis* and *Ephedripites*) have been correlated with warmth and aridity [26, 27, 48, 50, 58]. These sediments were thus deposited in a palaeoenvironment which was moist and humid in a warm coastal plain under arid/semi-arid climate condition.

## 6. Source rock evaluation

Evaluation of source rocks for their hydrocarbon potential is essential in exploration processes. To evaluate the hydrocarbon source potential of the Takoradi 11-1 well, samples were subjected to Rock Eval pyrolysis. Four parameters were acquired. These are  $S_1$ , free hydrocarbons;  $S_2$ , pyrolyzed hydrocarbons from the cracking of kerogen;  $S_3$ , quantity of  $CO_2$  released and  $T_{max}$ , the temperature at which most of the hydrocarbons were produced. These parameters were used to calculate the following: Oxygen Index [OI =  $(S_3/TOC) \times 100$ ], Hydrogen index [HI =  $(S_2/TOC) \times 100$ ], Production index [PI =  $S_1 / (S_1 + S_2)$ ]. The three main factors for evaluating the potential of a rock to produce petroleum are:

- Potential quantity of produced hydrocarbon which is based on  $S_1$ ,  $S_2$ , and TOC.
- Hydrogen type index which is based on HI, and  $S_2/S_3$  ratio.
- Thermal maturity for petroleum generation which is based on PI and  $T_{max}$  [42]. Table 4 below shows the standard guidelines for interpreting source rock quantity, quality and maturation, and commonly used Rock-Eval parameters.

Table 4 Guidelines for interpreting source rock quantity, quality and maturation, and commonly used Rock-Eval parameters [17-18, 20, 41, 42, 56]

Quantity	TOC	$S_1$ (mg HC/g rock)	$S_2$ (mg HC/g rock)
Poor	<0.5	<0.5	<2.5
Fair	0.5-1	0.5-1	2.5-5.0
Good	1-2	1-2	5-10
Very Good	2-4	2-4	10-20
Excellent	>4	>4	>20
Quality	HI (mg HC/g TOC)	$S_2/S_3$	Kerogen Type
None	<50	<1	IV
Gas	50-200	1-5	III
Gas and Oil	200-300	5-10	II/III
Oil	300-600	10-15	II
Oil	>600	>15	I



Maturation	Ro (%)	Tmax (°C)	TAI
Immature	0.2-0.6	<435	1.5-2.6
Early Mature	0.6-0.65	435-445	2.6-2.6
Peak Mature	0.65-0.9	445-450	2.7-2.9
Late Mature	0.9-1.35	450-470	2.9-3.3
Post Mature	>1.35	>470	>3.3

## 6.1 Organic richness and hydrocarbon generation potential

The organic richness and potential of a rock sample is evaluated by measuring the amount of total organic carbon TOC in the whole rock and pyrolysis derived  $S_2$  of the rock samples [57]. Carbonates and shales are considered hydrocarbon source if TOC exceeds 0.3 and 0.5%, respectively [41, 52]. The source rock potential has been identified according to the classification scheme of [9] shown below in Table 5.

Table 5 Classification of organic matter quantity and source rock potential

Quantity	TOC wt%	$S_2$
Poor	0 – 0.5	0 – 1
Fair	0.5 – 1	1 – 5
Good	1 – 2	5 – 10
Very Good	2 – 4	10 – 20
Excellent	>4	>20

Samples from the Takoradi 11-1 well have an average TOC of 0.83 wt% and  $S_2$  of 1.32 mg/g which indicate fair source rocks (Table 5, Fig. 5).

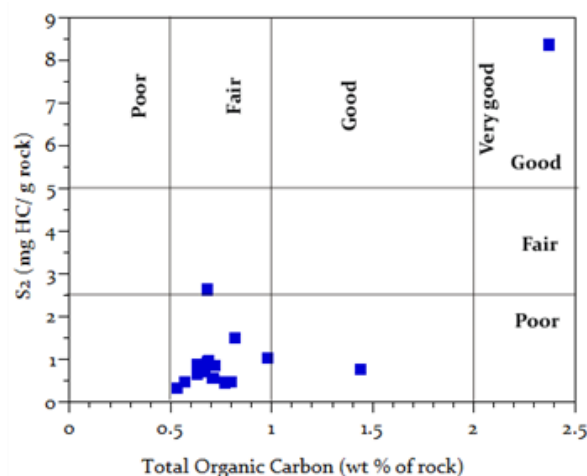


Figure 5 Plot of  $S_2$  versus TOC indicating hydrocarbon potential and source rock efficiency

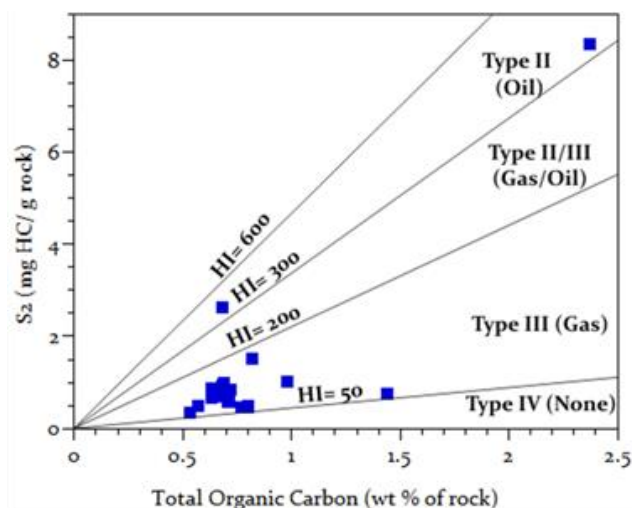


Fig. 6. Plot of  $S_2$  versus TOC indicating the kerogen types of the studied samples.

The plot of  $S_2$  versus TOC and determining the regression equation is the best method for analyzing the true average HI and measuring the adsorption of hydrocarbons by the rock matrix [40]. The analyzed samples from the well gave an average HI of 134 mg HC/ g TOC, thus falling in the range of gas prone kerogen (Fig. 6)

The plot of HI versus TOC (Fig. 7) presents the relationship between generation potential and the kerogen types present. The TOC results show that most of the samples from the well generally have a fair generative potential and supports the presence of a dominant type III kerogens (gas - prone).

Tissot *et al.* [52] proposed a genetic potential ( $GP = S_1 + S_2$ ) for the classification of source rocks. According to their classification scheme, rocks having GP of less than 2 mg HC/ g rock correspond to gas-prone rocks or non-generative ones, 2 - 6 mg HC/ g rock are moderate

source rocks with fair gas/oil potential, and GP greater than 6 mg HC/ g rock are good source rocks. The samples in well Takoradi 11 – 1 have poor to fair organic carbon content and poor to fair genetic potential (0.36 – 8.55; ave 1.37) (Fig. 8) and thus the rocks can be described as predominantly gas - prone source rocks.

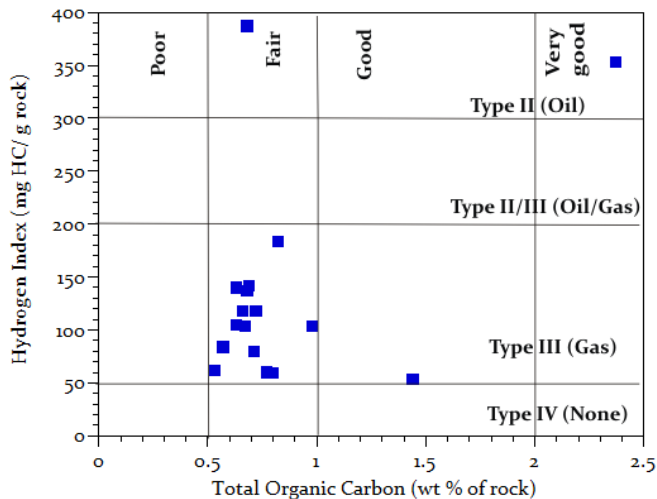


Fig. 7. Plot of Hydrogen index versus TOC indicating amount of kerogen types and generation potential.

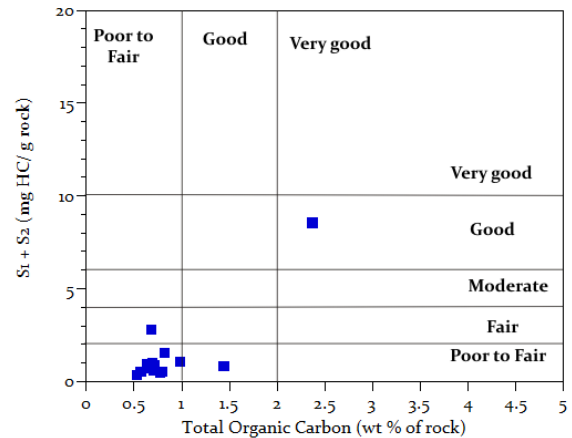


Fig. 8. Plot of  $S_1 + S_2$  versus TOC showing the Genetic potential of rocks.

## 6.2 Kerogen type and maturity

Kerogen types can be identified by optical methods and by organic geochemical methods where values of elemental analysis of C, O, and H are plotted on a Van Krevelen diagram which defines four types of kerogen [32, 42, 53]. The organic matter type is an important parameter in evaluating source rock potential and has a first order control on the nature of the hydrocarbon products. Kerogen types can also be distinguished by plotting HI versus OI from Rock-Eval pyrolysis on a modified Van Krevelen diagram [18]. The kerogen designation is based entirely on HI [28] but the kerogen quality and maturity are determined by plotting HI versus Tmax rather than HI versus OI (Fig. 9). This eliminates the use of OI as a kerogen type indicator. Fig. 9 shows that the samples are predominantly Type III kerogens (gas prone). The HI values (53 – 142; and 353 and 387 for two samples) for the samples with average HI of 135 HC/g TOC also suggests predominant kerogen Type III.

The plot of HI versus Tmax is routinely used to depict both the type of kerogen present in a source rock, in order to avoid the influence of OI for determining kerogen type [28]. Fig.10 shows that the samples from Takoradi well 11-1 contain mainly gas-prone Type III kerogens. The inferred vitrinite reflectance (0.52 – 0.77; ave 0.65) data in Appendix 1 indicates that most of the samples are within the early mature zone.

Thermal maturity is influenced by source rock organic matter type and the presence of excess free hydrocarbon together with the other factors like mineral matter, content, depth of burial and age [56]. Data indicators for maturity includes Tmax, Production Index (PI) and Vitrinite Reflectance. The increase of maturity level of organic matter corresponds to an increase in Tmax particularly for immature samples.  $PI = \{S_1 / [S_1 + S_2]\}$  is a valuable method for indicating the thermal maturity of organic matter. The following relations between Tmax and PI are observed:

- Immature organic matter has Tmax and PI values less than 430°C and 0.10, respectively;
- Mature organic matter has a range of 0.1– 0.4 PI. At the top of oil window, Tmax and PI reach 460°C and 0.4, respectively;
- Mature organic matter within the wet gas-zone has PI values greater than 0.4; and

- Post-mature organic matter usually has a high PI value and may reach 1.0 by the end of the dry-gas zone [7, 41, 42].

Most of the samples from the well have  $T_{max} > 435^{\circ}\text{C}$  and  $<0.1$  PI thereby making them early mature and indigenous samples, yet to enter the hydrocarbon generation zone (Fig. 11).

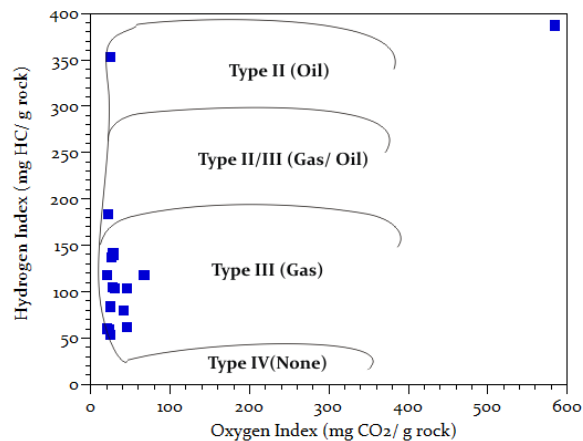


Fig. 9 Modified Van Krevelen diagram indicating the Kerogen types of the studied samples.

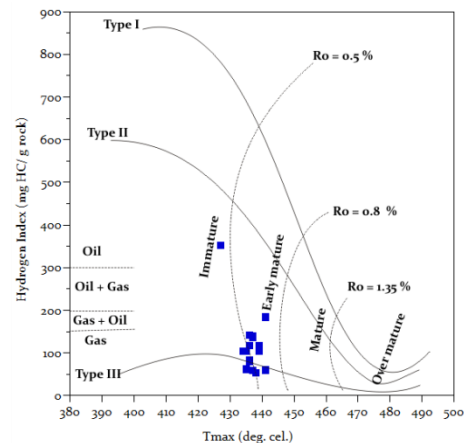


Fig. 10 Plot of Hydrogen Index versus  $T_{max}$  showing the relationship between kerogen types and maturity levels.

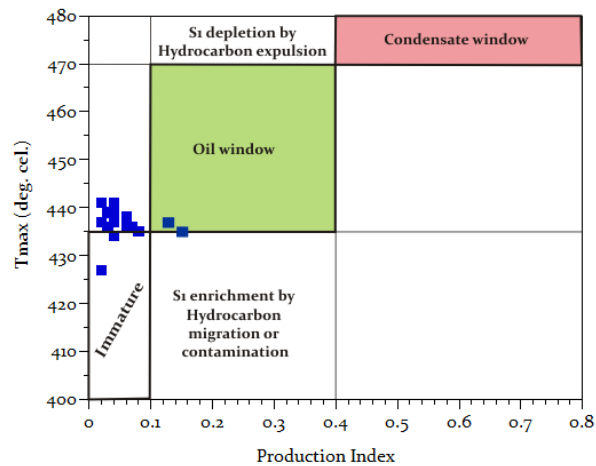


Fig. 11 Plot of  $T_{max}$  versus Production Index showing the hydrocarbon-generation zone.

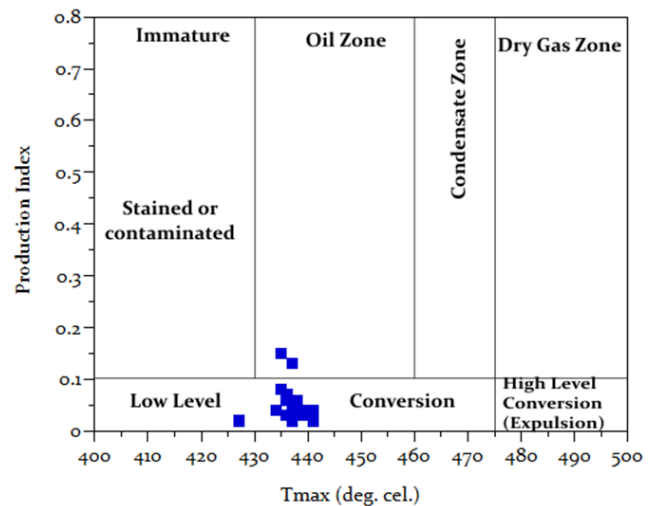


Fig.12 Plot of Production Index versus  $T_{max}$  showing levels of kerogen conversion and maturity.

Plot of production index versus  $T_{max}$  (Fig. 12) indicate that rock samples from Takoradi 11-1 well has a poor to fair source rock quality of early maturity with low level of conversion and no contaminated or migrated hydrocarbons.

### 6.3 Expulsion ability

$S_1$  represents the free hydrocarbons already present in the sample, and  $S_2$  represents the hydrocarbons generated during pyrolysis. Free hydrocarbons are those already produced from organic material and will be proportional to the Total Organic Carbon (TOC) of any given source rock. The Ocean Drilling Program uses  $S_1/\text{TOC}$  of 1.5, to determine the presence of indigenous versus migrated or non-indigenous hydrocarbon levels [28].

The plot of  $S_1$  versus TOC (Figure 13) shows that all source rocks contain an expected level of  $S_1$  hydrocarbons for their given TOC, and are hence predominantly indigenous.

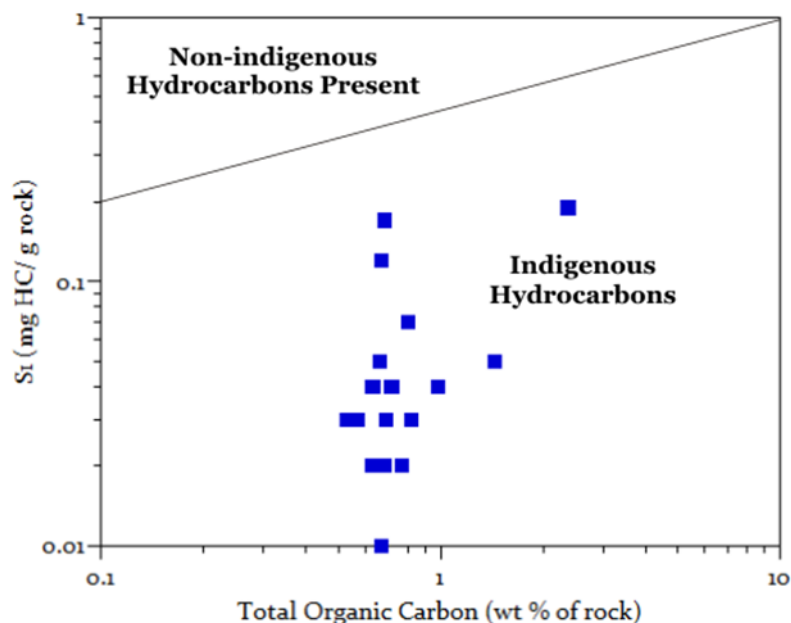


Fig. 13  $S_1$  versus TOC as an indicator of indigenous and non-indigenous hydrocarbons

## 7. Conclusion

The organic geochemical analysis of the studied samples show a fair to moderate organic matter (0.53 – 2.37 wt% TOC) which is gas prone.

Palynofacies analyses reflect kerogen type III which were deposited in three palynofacies associations: PA-1 which is deposition in distal mud-dominated oxic shelf conditions; PA-2 deposition in a distal dysoxic – anoxic (outer) shelf condition and PA-3 distal dysoxic – anoxic (inner) shelf environment. Deductions from palynomorph assemblages which are characteristic of the Albian – Cenomanian elaterate province, reveal deposition in a moist, humid coastal plain under warm arid/semiarid tropical condition.

Organic geochemical analysis indicate mainly type III kerogen, immature to early mature source rock with fair hydrocarbon generation potential to generate gas.

## Acknowledgement

The authors acknowledge GNPC for providing data for the study. Our special thanks goes to Mr. Ebenezer Apesegah, Manager in charge of Geology, GNPC for being supportive during the study.

## References

- [1] Abubakar MB, Luterbacher HP, Ashra, AR, Ziedner R, Maigari AS. Late Cretaceous palynostratigraphy in the Gongola Basin (Upper Benue Trough, Nigeria). *Journal of African Earth Science* 2011; 60:19-27.
- [2] Adda, GW, Atta-Peters, D, Ben-Awuah, J. Burial History, Thermal Maturity and Petroleum Generation History of the Lower Paleozoic Petroleum System in the Saltpond Basin, Offshore Ghana. *Search and Discovery* 2015; Article # 10709.
- [3] Alaug, AS. Hydrocarbon potential of the Upper Cretaceous succession at well 16/U-1, offshore Qamar Basin, Eastern Yemen. *Journal of Petroleum Geology* 2011; 34:1, 87 – 108.
- [4] Alaug, AS, Mahmoud, MS, Deaf, AS, Al-Ameri, TK. Palynofacies, Organic Geochemical analyses and hydrocarbon potential of some upper Jurassic-Lower Cretaceous rocks, the Sabatayn-1 well, Central Yemen. *Arabian Journal of Geosciences* 2014; 7: 2515-2530.

- [5] Asiedu, DK, Hegner, E, Rocholl, A, Atta-Peters, D. Provenance of Late Ordovician to Early Cretaceous sedimentary rocks from Southern Ghana as inferred from Nd isotopes and trace elements: *Journal of African Earth Science* 2005; 41: 4, 318-319.
- [6] Atta-Peters, D, Salami, MB. Aptian-Maastrichtian palynomorphs from the offshore Tano Basin, Western Ghana. *Journal of African Earth Sciences* 2006; 46: 379-394.
- [7] Bacon, C. A., Calver, C. R., Boreham, C. J., Leaman, D. E., Morrison, K. C., Revill, A. T. Volkman, J. K. The petroleum potential of onshore Tasmania: a review. *Mineral Resources Tasmania, Geological Survey Bulletin* 2000; 71-79.
- [8] Bansah, S, Gon Qin, Nyantakyi, EK, Borkloe, JK, Awuni, LA. Geochemical characterization of potential source rock of the Central (Saltpond) Basin, Ghana. *International Journal of Oil, Gas and Coal Engineering* 2014; 2: 2, 19-27.
- [9] Baskin, DK. Atomic H/C Ratio of Kerogen as an Estimate of Thermal Maturity and Organic Matter Conversion. *American Association of Petroleum Geologists Bull.*, 1997; 81:1437-1450.
- [10] Batten, DJ. The use of transmitted light microscope on sedimentary organic matter for valuation of hydrocarbon source potential. IV Int. Palynol, Conf., Lucknow (1976-77).1980; 2, 589-594.
- [11] Batten, DJ. Palynofacies, organic maturation and source potential for petroleum. In: Brooks J. (Ed), *Organic maturation studies and fossil fuel exploration*. Academic Press, London; 1981, 201 – 223.
- [12] Batten, DJ. Identification of amorphous sedimentary organic matter by transmitted light microscopy. In Brooks, J. (Ed.), *Petroleum geochemistry and exploration of Europe*, Geological Society Special Publication 12, Blackwell Science, Oxford; 1983, 275 – 287.
- [13] Batten, DJ, Uwins, PJR. Early–Late Cretaceous (Aptian–Cenomanian) Palynomorphs. *Journal of the British Micropalaeontological Society*, 1985; 4:1, 151-168.
- [14] Braspetro International S.A. Saltpond Field Reservoir Engineering Study; 1986.
- [15] Dino, R, Pocknall, DT, Dettman, ME. Morphological and ultrastructure of elater-bearing pollen from Albian to Cenomanian of Brazil and Equador: implications for botanical affinity. *Review of Palaeobotany and Palynology*, 1999; 105: 211–235.
- [16] El Beialy, El-Soughier, M, El Atfy, H, Mohsen, SA. Palynostratigraphy and paleoenvironmental significance of the Cretaceous succession in the Gebel Rissu-1 well, north Western Desert, Egypt. *Journal of African Earth Science*, 2011; 59: 215-226.
- [17] Epstein, AG, Epstein, JB, Harris, LD. Conodont color alteration - an index to organic metamorphism: U.S. Geological Survey Professional Paper, 1977; 995: 27 pp.
- [18] Espitalié, J, Laporte, L J, Madec, M, Marquis, F, Leplat, P J, Boutefeu, A. Méthode rapide de caractérisation des roches mères de leur potentiel pétrolier et de leur degré devolution. *Rev. Inst. Franc. Pétrole*, 1977; 32: 32-42.
- [19] Espitalié, J, Marquis F, Barsony, I. Geochemical logging, In: Voorhees KJ (ed) *Analytical pyrolysis: techniques and applications*. Butterworth, London, 1984; p. 276–304.
- [20] Fowler, M, Snowdon, L, Stasiuk, V. Applying petroleum geochemistry to hydrocarbon exploration and exploitation. *American Association of Petroleum Geologists Short Course Notes*, June 18-19, 2005; Calgary, Alberta, 224 pp.
- [21] Ghasemi-Nead, E, Head, JM, Naderi, M. Palynology and petroleum potential of the Kazhdumi Formation (Cretaceous: Albian-Cenomanian) in the South Pars field, northern Persian Gulf. *Marine and Petroleum Geology*, 2009; 26: 805-816.
- [22] Ghana National Petroleum Corporation. Saltpond reservoir geological study: GNPC Exploration Department, Tema - Ghana, 1993; 2 pp.
- [23] Herngreen, GFW. Palynology of the Albian–Cenomanian strata of borehole 1-QS-1-MA. *State of Maranhao, Brazil. Pollen et Spores*, 1975; 15: 3–4), 515–555.
- [24] Herngreen, GFW. Palynology of Middle and Upper Cretaceous strata in Brazil. *Mededelingen Rijks Geologische Dienst, N.S.*, 1975; 26:3, 39–91.

- [25] Herngreen, GFW. Cretaceous sporomorph provinces and events in the equatorial region. *Zentralblatt für Geologie und Paläontologie* 1996. 1998; (11/12), 1313–32.
- [26] Herngreen, GFW, Dueñas-Jimenez, H. Dating of the Cretaceous Une Formation, Colombia and the relationship with the Albian–Cenomanian Africa–South American microfloral province. *Review of Paleobotany and Palynology*, 1990; 66: 345–359.
- [27] Herngreen, GFW, Kedves, M, Rovnina, LV, Smirnova, SB. Cretaceous palynofloral provinces: a review. In: Jansonius, J, McGregor, DC. (Eds.), *Palynology: principles and applications*, Vol. 3. American Association of Stratigraphic Palynologist Foundation, 1996; 1157–1188.
- [28] Hunt, JM. *Petroleum geology and geochemistry*, 2<sup>nd</sup> edition: WH Freeman and Company, New York, 2000; 743 pp.
- [29] Ibrahim, MIA. Late Albian – middle Cenomanian palynofacies and palynostratigraphy, Abu Gharadig-5 well, Western Desert, Egypt. *Cretaceous Research*, 2002; 23: 775–788.
- [30] Ibrahim, MIA, Al-Saad, H, Kholeif, SE. Chronostratigraphy, palynofacies, source rock potential, and organic thermal maturity of Jurassic rocks of Qatar. *GeoArabia*, 2002; 7: 675 – 696.
- [31] IHS. Saltpond Basin, Ghana; 1999.
- [32] Jacobson, SR. Petroleum source rocks and organic facies. In Merrill, RK. (ed), *Source and migration processes and evaluation techniques: American Association of Petroleum Geologists Handbook of Petroleum Geology*, 1991; 1–11.
- [33] Jardiné, S. Spore a` expansions en form d`elateres du Cretace moyen d'Afrique occidentale. *Review of Paleobotany and Palynology*, 1967; 1: 235–258.
- [34] Jardiné, S, Magloire, L. *Palynologie et stratigraphie du Crétacé des bassins du Sénégal et d'Côte d'Ivoire*. Mémoire Bureau Recherche Géologie et Minéralogie, 1965; 32 : 187–245.
- [35] Kanehara, Y. Structural styles and hydrocarbon potential of the offshore Ghana. *Sekiyo Gijutsu Kyokaishi (Journal Japanese Association of Petroleum Technology)*, 1989; 54: 1, 84–91.
- [36] Kholeif, SH, Ibrahim, MI. Palynofacies analysis of inner continental shelf and middle slope sediments offshore Egypt, Southeastern Mediterranean. *Geobios*, 2010; 43: 333 – 347.
- [37] Kjemperud, A., Agbesinyale, W., Agdestein, T., Gustafsson, C., and Yüklér, A. Tectono-stratigraphic history of the Keta Basin, Ghana with emphasis on late erosional episodes; In R. Cumelle, (ed.), *Geologie Africaine -1st Colloque de stratigraphie et de paleogeographie des bassins sedimentaires ouest-Africans*, 2nd Colloque Africa in de Micropaleontologie, Libreville, Gabon, May 6 – 8, 1991: *Elf Aquitaine Memoir*, 1992; 13: p. 55–69.
- [38] Mahmoud, MS, Deaf, AS. Cretaceous Palynology (spores, pollen and dinoflagellate cysts) of the Siqueifa 1-X Borehole, Northern Egypt. *Rivista Italiana di Paleontologia e Stratigrafia*, 2007; 133: 2, 203–221.
- [39] Muller, J, de Di Giacomo, E, van Erve, AW. A palynological zonation for the Cretaceous, Tertiary and Quaternary of Northern South America. *American Association of Stratigraphic Palynologist Contribution Series*, 1978; 19: 7–76.
- [40] Obaje NG, Wehner, H, Scheeder, G, Abubakar, MB, Jauro, A. Hydrocarbon prospectively of Nigeria's inland basins: organic geochemistry and organic petrology, *American Association of Petroleum Geologists Bulletin*, 2004; 88: 3, 325–353.
- [41] Peters, KE. Guidelines for evaluating petroleum source rock using programmed pyrolysis: *American Association of Petroleum Geologists Bulletin*, 1986; 70: 318–329.
- [42] Peters KE, Cassa, MR. Applied source rock geochemistry, in Magoon, L.B., and Dow, W.G., eds., *The petroleum system – from source to trap: American Association of Petroleum Geologists*, 1994; 60: 93–120.
- [43] Playford, G. Palynology of the Lower Cretaceous (Swan River) strata of Saskatchewan and Manitoba. *Paleontology*, 1971; 14: 4, 533–565.

- [44] Regali, MSP, Viana, CF. Late Jurassic–Early Cretaceous in Brazilian sedimentary basins: correlation with the international standard scale, Petrobras, Rio de Janeiro, 1989; 95 pp.
- [45] Schrank, E. Paleozoic and Mesozoic palynomorphs from northeast Africa (Egypt and Sudan) with special reference to late Cretaceous pollen and dinoflagellates. *Berliner Geowissenschaftliche Abhandlungen A*, 1987; 75: 1, 249–310.
- [46] Schrank, E. Palynology of the classic Cretaceous sediments between Dongola and Wadi Muqaddam, Northern Sudan. *Berliner Geowissenschaftliche Abhandlungen A*, 1990; 120: 1, 149–168.
- [47] Schrank, E. Paleoeological aspects of *Afropollis*/elaterate peaks (Albian- Cenomanian pollen) in the Cretaceous of Northern Sudan and Egypt. In: Goodman, DK, Clarke, RT. (Eds.), *Proceedings of the IX International Palynological Congress*, Houston, Texas, USA, 1996. American Association of Stratigraphic Palynologist Foundation, 2001; 201–210.
- [48] Schrank, E. Ibrahim, MIA. Cretaceous 9Aptian–Maastrichtian palynology of foraminifera dated wells (KRM-1, AG-18) in northwestern Egypt. *Berliner Geowissenschaftliche Abhandlungen A*, 1995; 177: 1–44.
- [49] Schrank, E, Mahmoud, MS. Palynology (pollen, spores and dinoflagellates) and Cretaceous stratigraphy of the Dakhla Oasis, central Egypt. *Journal of African Earth Science*, 1998; 26: 2, 167–193.
- [50] Schrank, E, Nesterova, EV. Palynofloristic changes and Cretaceous climates in northern Gondwana (NE Africa) and southern Laurasia. In: Thorweihe, Schandelmeier (Eds.). *Geoscientific Research in Northeast Africa*, 1993; 381–390.
- [51] Thusu, B, Van der Eem, JGLA. Early Cretaceous (Neocomian–Cenomanian) palynomorphs. In: Thusu, B, Owens, B. (Eds.), *Palynology of northeast Libya*. *Journal of Micropaleontology*, 1985; 4: 1, 131–150.
- [52] Tissot, BP, Welte, DH. *Petroleum formation and occurrence* (2nd edition) Berlin, Springer-Verlag, 1984.
- [53] Tissot, B, Durand, B, Espitalié, J, Combaz, A. Influence of the nature and diagenesis of organic matter in the formation of petroleum. *American Association of Petroleum Geologists Bulletin*, 1974; 58: 499–506.
- [54] Tyson, RV. Palynofacies analysis. In: Jenkins DJ(Ed), *Applied Micropaleontology*, Kluwer Academic publishers, Dordrecht, 1993; p. 153–191.
- [55] Tyson, RV. *Sedimentary Organic matter - Organic facies and palynofacies*. Chapman and Hall, London, 1995.
- [56] Traverse, A. *Paleopalynology*, Unwin Hyman, Boston, 1988.
- [57] Waples, D. W, Kamata, H, Suizu, M. The art of maturity modeling: Part 1. Finding a satisfactory geological model: *American Association of Petroleum Geologists Bulletin*, 1992; 76: 31–46.
- [58] Zavattieri, AN, Rosenfield, U, Volkheimer, W. Palynofacies analysis and sedimentary environment of Early Jurassic coastal sediments at the southern border of the Neuquen Basin, Argentina. *Journal of South American Earth Sciences*, 2008; 25: 277 – 245.



## Supplements

### EXPLANATION OF PLATES

#### PLATE I

All Figures x 800

Fig.

- A. *Appendicisporites jansonii* Pocock, 1962
- B. *Triplanosporites* sp.
- C. *Gnetaceaepollenites ?irregularis*
- D. *Retimonocolpites variplicatus* Schrank and Mahmoud, 1998
- E. *Gleicheniidites senonicus* Ross, 1949
- F. *Galaeocornea causea* Stover, 1963
- G. *Cyberosporites pannaceus* (Brenner) Srivastava, 1977
- H. *Cyathidites australis* Couper, 1953
- I. *Elaterosporites africanensis* Herngreen, 1973
- J. *Cretacaeisporites polygonalis* (Jardiné et Magloire) Herngreen, 1973
- K. *Chomotriletes minor* (Kedves) Pocock 1970
- L. *Elateropollenites jardinei* Herngreen, 1973

#### PLATE II

All Figures x 800

Fig.

- A. *Classopollis torsus* (Ressinger) Couper, 1958
- B. *Elaterosporites klaszii* (Jardiné et Magloire) Jardine, 1967
- C. *Reyrea polymorphus* Herngreen, 1973
- D. *Ephedripites irregularis* Herngreen, 1973
- E. *Multiplicisphaeridium ramusculosum* (Deflandre) lister, 1970
- F. *Appendicisporites bilateralis* C. Singh, 1971
- G. *Ephedripites* sp
- H. *Afropollis jardinus* Doyle et al., 1982
- I. *Sofrepites legouxiae* Jardine, 1967
- J. *Veryhachium lairdi* (deflandre) Deunff, 1958
- K. *Elaterosporites protensus* (Stover) Jardine, 1967
- L. *Cicatricosisporites hallei* Delcourt and Sprumont, 1955

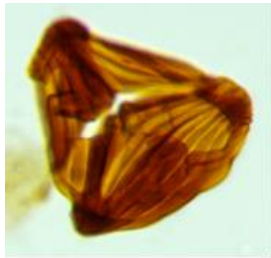
#### PLATE III

All Figures x 200

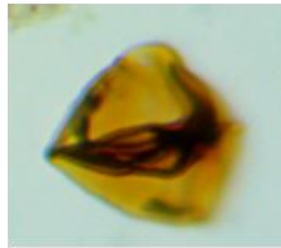
Fig.

- A, B. Palynofacies Assemblage 1 (PA-1). Relatively equal dominance of AOM and palynomorphs with phytoclasts.
- C, D. Palynofacies Assemblage 2 (PA-2). AOM dominant
- E, F. Palynofacies Assemblage 3 (PA-3). Palynomorphs dominant with phytoclast and AOM.

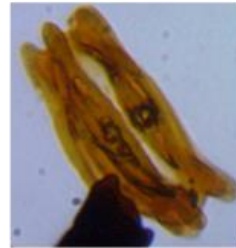
**PLATE I**



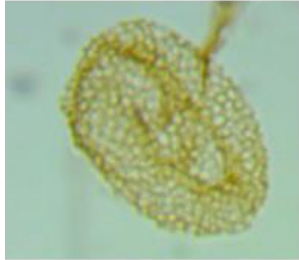
**A**



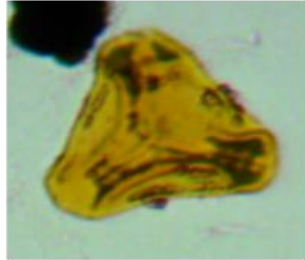
**B**



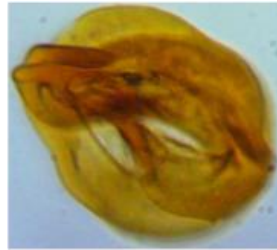
**C**



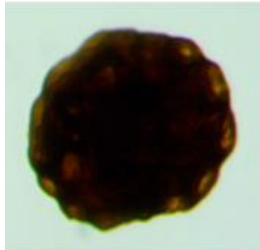
**D**



**E**



**F**



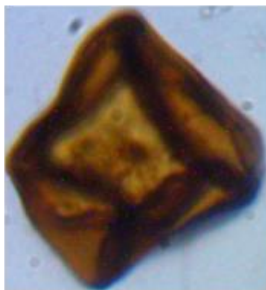
**G**



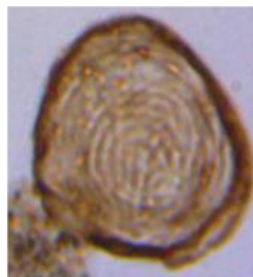
**H**



**I**



**J**



**K**

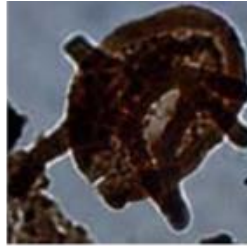


**L**

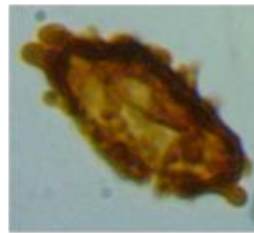
**PLATE II**



**A**



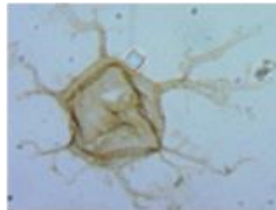
**B**



**C**



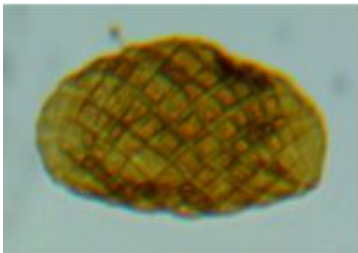
**D**



**E**



**F**



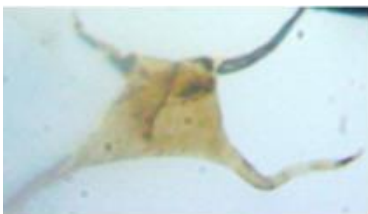
**G**



**H**



**I**



**J**

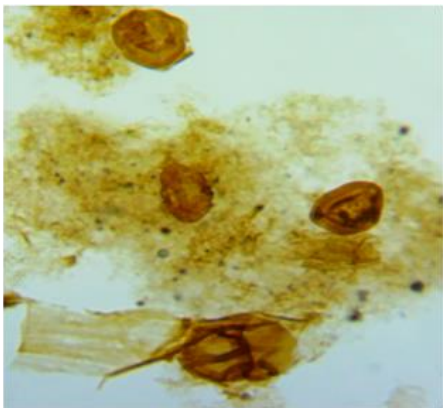


**K**

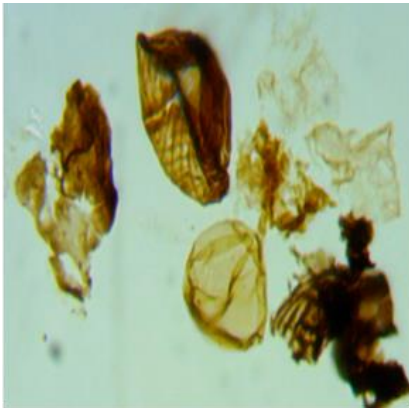


**L**

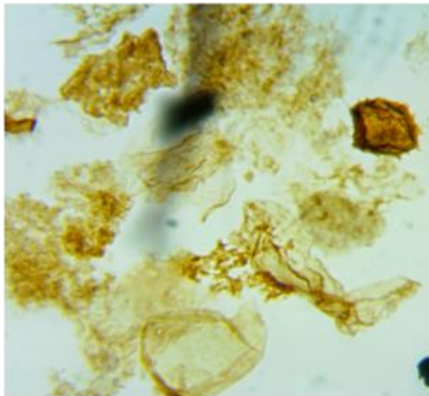
**PLATE III**



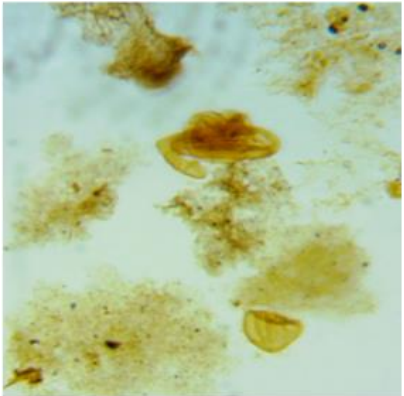
**A**



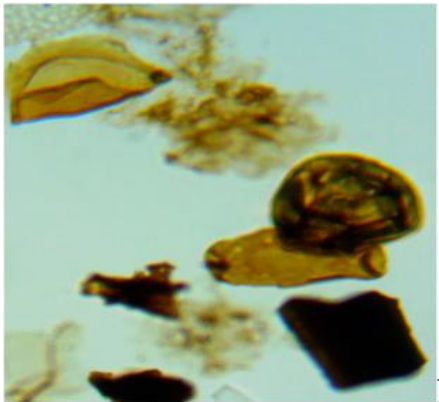
**B**



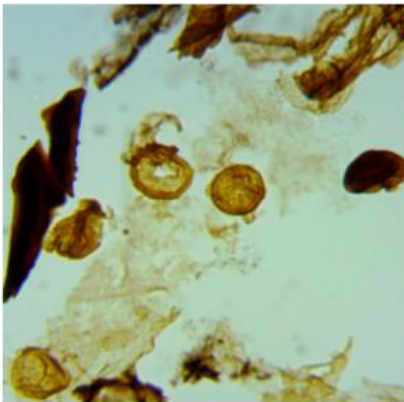
**C**



**D**



**E**



**F**

# Appendix 1 Relative Percentage Abundance of SOM and Palynomorphs

DEPTH/FT	AOM	PHYTOCLASTS	OPAQUES	PALYNOMORPHS
5430	40.29	14.29	10.00	35.43
5520	34.29	19.43	12.86	33.43
5610	32.86	20.00	10.00	37.15
5700	40.86	17.14	11.14	30.86
5790	23.43	18.29	15.43	42.86
5880	31.43	22.29	13.71	32.57
5970	25.71	25.43	15.71	33.14
6060	29.14	31.43	10.00	29.44
6150	26.57	29.14	12.00	32.29
6240	36.86	18.57	10.00	34.57
6330	21.43	27.14	8.860	42.57
6420	28.29	28.00	5.430	38.29
6510	20.00	32.29	8.570	39.07
6600	22.57	24.00	8.860	41.43
6690	21.71	23.43	7.710	47.14
6780	28.00	28.57	5.710	37.71
6870	28.00	28.29	6.290	37.43
6960	21.14	32.00	6.860	42.00
7050	19.43	29.14	7.430	42.00
7140	10.29	33.43	8.570	47.71
7230	37.43	22.29	7.710	32.57
7320	40.29	21.43	6.000	32.29
7410	17.43	34.29	8.290	40.00
7500	24.86	27.14	14.29	42.29
7590	29.14	25.14	5.140	40.57
7680	32.29	20.00	5.430	42.29
7770	33.71	26.57	8.860	30.86
7860	33.43	29.14	11.14	26.29
7950	31.71	25.71	8.290	34.29
8040	30.29	21.71	14.57	30.86
8130	34.29	21.71	14.57	29.44
8220	28.86	28.29	10.57	32.29
8310	33.43	28.57	11.43	26.57
8400	30.57	31.43	5.140	32.86
8490	28.00	30.57	7.140	34.29
8580	31.43	30.00	7.710	30.86
8670	26.00	33.71	9.430	30.86
8760	23.14	34.57	10.86	31.43
8850	26.29	26.86	8.570	38.29
8940	31.71	23.71	8.290	36.29
9030	32.86	22.86	8.570	35.71
9120	34.29	22.00	9.710	34.00
9210	36.57	26.29	7.430	29.71
9300	30.86	28.57	11.43	29.14
9390	33.71	27.43	10.29	28.57
9480	40.86	29.71	11.14	18.29
9570	40.86	28.29	9.710	21.14
9660	39.71	30.86	16.86	12.57
9750	49.70	25.40	13.40	11.50

**Appendix 2 Relative Percentage Abundance of SOM and Palynomorphs used for Ternary Plot**

DEPTH/FT	AOM	PHYTOCLASTS	PALYNOMORPHS
5430	40	25	35
5520	35	32	33
5610	33	30	37
5700	41	28	31
5790	23	34	43
5880	31	36	33
5970	26	41	33
6060	29	41	29
6150	27	41	32
6240	37	29	35
6330	21	36	43
6420	28	33	38
6510	20	41	39
6600	23	33	41
6690	22	31	47
6780	28	34	38
6870	28	35	37
6960	21	39	42
7050	19	37	42
7140	10	42	48
7230	37	30	33
7320	40	27	32
7410	17	43	40
7500	25	41	42
7590	29	30	41
7680	32	25	42
7770	34	35	31
7860	33	40	26
7950	32	34	34
8040	30	36	31
8130	34	36	29
8220	29	39	32
8310	33	40	27
8400	31	37	33
8490	28	38	34
8580	31	38	31
8670	26	43	31
8760	23	45	31
8850	26	35	38
8940	32	32	36
9030	33	31	36
9120	34	32	34
9210	37	34	30
9300	31	40	29
9390	34	38	29
9480	41	41	18
9570	41	38	21
9660	40	48	13
9750	50	39	12

**Appendix 3 WELL: TAKORADI 11-1**

Company: GNPC

LOCATION: OFFSHORE GHANA

Depth (ft)	TOC (wt % of rock)	S1 (mg HC/ g rock)	S2 (mg HC/ g rock)	S3 (mg CO2/ g rock)	S2/S3 (mg HC/ mg CO2)	Genetic Potential (mg HC/ g rock)	Production Index	Hydrogen Index (mg HC/ g rock)	Oxygen Index (mg CO2/ g rock)	Ro (%)	Tmax (°C)	S1/ TOC (mg HC/ g rock)
4350-4440	2.37	0.19	8.36	0.6	13.93	8.55	0.02	353	25	0.53	427	0.08
5640-5730	0.67	0.01		0.2					30			0.01
6810-6900	0.69	0.03	0.98	0.19	5.16	1.01	0.03	142	28	0.69	436	0.04
6990-7080	0.53	0.03	0.33	0.24	1.38	0.36	0.08	62	45	0.67	435	0.06
7080-7170	0.63	0.04	0.88	0.18	4.89	0.92	0.04	140	29	0.71	437	0.06
7260-7320	0.72	0.04	0.85	0.15	5.67	0.89	0.04	118	21	0.74	439	0.06
7320-7410	0.82	0.03	1.51	0.18	8.39	1.54	0.02	184	22	0.78	441	0.04
7410-7500	0.71	0.04	0.57	0.29	1.97	0.61	0.07	80	41	0.69	436	0.06
7500-7590	0.63	0.02	0.66	0.17	3.88	0.68	0.03	105	27	0.74	439	0.03
7590-7680	0.68	0.02	0.93	0.18	5.17	0.95	0.02	137	26	0.71	437	0.03
7860-7950	0.98	0.04	1.02	0.29	3.52	1.06	0.04	104	30	0.65	434	0.04
7950-8040	1.44	0.05	0.76	0.36	2.11	0.81	0.06	53	25	0.72	438	0.03
8040-8130	0.66	0.05	0.78	0.44	1.77	0.83	0.06	118	67	0.69	436	0.08
8220-8310	0.8	0.07	0.47	0.18	2.61	0.54	0.13	59	23	0.71	437	0.09
8310-8400	0.77	0.02	0.46	0.16	2.88	0.48	0.04	60	21	0.78	441	0.03
8550-8610	0.67	0.12	0.7	0.3	2.33	0.82	0.15	104	45	0.67	435	0.18
8700-8790	0.57	0.03	0.48	0.14	3.43	0.51	0.06	84	25	0.69	436	0.05
9980-10020	0.68	0.17	2.63	3.97	0.66	2.8	0.06	387	584			0.25
Minimum	0.53	0.01	0.33	0.14	0.66	0.36	0.02	53	21	0.526	427	0.01
Average	0.83	0.06	1.32	0.46	4.10	1.37	0.06	134.70	61.89	0.70	436.5	0.07
Maximum	2.37	0.19	8.36	3.97	13.93	8.55	0.15	387	584	0.778	441	0.25